C. R. Mecanique 342 (2014) 292–298

Contents lists available at ScienceDirect

Comptes Rendus Mecanique

www.sciencedirect.com

Frontiers of micro and nanomechanics of materials: Soft or amorphous matter, surface effects

Indentation-triggered pattern transformation in hyperelastic soft cellular solids

Ke-Lin Chen, Yan-Ping Cao *, Man-Gong Zhang, Xi-Qiao Feng

Institute of Biomechanics and Medical Engineering, Department of Engineering Mechanics, Tsinghua University, Beijing, 100084, China

ARTICLE INFO

Article history:
Received 6 May 2013
Accepted 20 October 2013
Available online 24 April 2014

Keywords:
Hyperelastic cellular solid
Indentation
Pattern transformation

ABSTRACT

This paper explores indentation-triggered microstructural instability in hyperelastic cellular solids through combined experimental, numerical, and theoretical efforts. The results demonstrate that when the indentation depth is greater than a critical value, local instability occurs and further propagates into a rectangular region beneath the indenter. The width of the rectangular region scales with the contact width, and we propose a simple scaling relation to estimate the maximum depth to which the instability can propagate based on the elastic contact theory. The results reported here may find such applications as in the integrity evaluation of soft cellular materials and structures and the development of advanced functional materials with unique optical, acoustic and wetting properties.

1. Introduction

Soft materials with small-scale periodic cellular structures have a wide variety of technologically important applications, ranging from photonic or phononic band-gap materials, microfluid networks, self-healing materials to scaffolds in tissue engineering [1–6]. Due to their low elastic moduli and large deformation ability, elastic instability of microstructures may occur in the soft hyperelastic cellular materials under loading. Understanding the microstructure instability is of great importance. For instance, in the use of soft cellular materials as components of microdevices, stable microstructure is usually required to guarantee their desired performance and functions. The occurrence and propagation of the instability (e.g., caused by the contact with other harder components) may represent the failure of the system. On the other hand, microstructural instability can be utilized in some other circumstances. For example, a recent interesting study of Mullin et al. [7] found that uniaxial compression can trigger dramatic pattern transformations in certain classes of simple periodic structures, foreseeing a route for creating metamaterials with transformative photonic/phononic or hydrophobic/hydrophilic attributes [7]. Although historically numerous studies have been carried out on the deformation behavior of cellular solids [8–11], investigation on the microstructural instability of hyperelastic cellular solids with the focus on the development of metamaterials is only recently pursued [7,12]. Different from simple compression, deformation induced by local contact pressure (e.g., under contact or indentation load) varies along the depth according to elastic contact theory [7]. Thus it is expected that indentation may trigger pattern transformation with controllable spatial gradient in a periodic cellular hyperelastic material. This method could be particularly useful for the development of some photonic crystals, surface patterns with unique wetting properties, and scaffolds for tissue engineering [14].

* Corresponding author. Tel.: +86 10 62772520.
E-mail address: caoyanping@tsinghua.edu.cn (Y.-P. Cao).

http://dx.doi.org/10.1016/j.crme.2014.01.011
1631-0721/

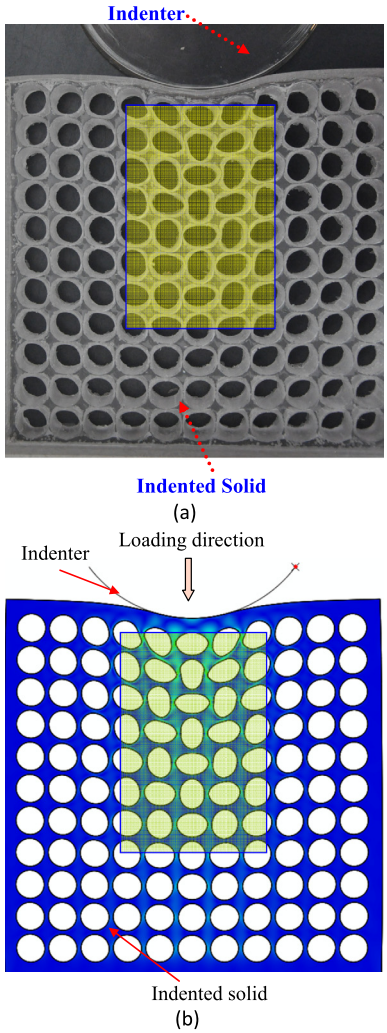

Fig. 1. (Color online.) Indentation-triggered microstructural instability in an elastomeric cellular solid. (a) A desktop experiment; (b) the result of post-buckling analysis.

Based on the above considerations, we here explore the indentation problem of hyperelastic materials with periodic cellular structures. Indentation has been widely adopted in material characterizations and nano-imprinting in recent years [15,16], which currently can be easily performed with commercial equipments at different length scales. In the literature, a number of authors have investigated the indentation of cellular solids [17,18], where the matrix material is assumed to be elastoplastic. However, indentation-induced microstructural instability and its propagation in **hyperelastic** cellular solids has not been investigated. In this study, our attention is paid to two interesting issues, i.e., how the local instability of microstructures occurs under contact load imposed by indentation and how it propagates in the material. To this end, we performed a desktop-scaled indentation experiment of a soft material consisting of circular holes using a cylindrical indenter and carried out nonlinear finite-element analysis to simulate the plane-strain indentation. A model is further devised to understand the underlying physics based on the elastic contact theory [13].

2. Experiments

In our desktop experiment, a mold consisting of a square array of 11×11 identical cylinders was prepared. Polydimethylsiloxane (PDMS) was prepared by mixing a degassed elastomer base and a crosslinker in a ratio of 10:1 w/w. The pre-polymerized mixture was filled in the mold and cured at 60 °C for 8 h. When the PDMS had become a solid state, the cylinders were taken out and a specimen consisting of 11×11 circular holes was obtained. The sample was 190 mm long, 190 mm wide, and 20 mm thick. All holes had the same diameter of 14 mm, and the center-to-center spacing was 16 mm. The indentation test was performed by using a glass cylinder with the diameter of 128 mm, which is sufficiently hard to be considered as rigid. Fig. 1a shows the deformation in the indented sample when the indentation depth was around 10 mm. Indentation-induced local microstructural instability could be evidenced, which further triggered distinct

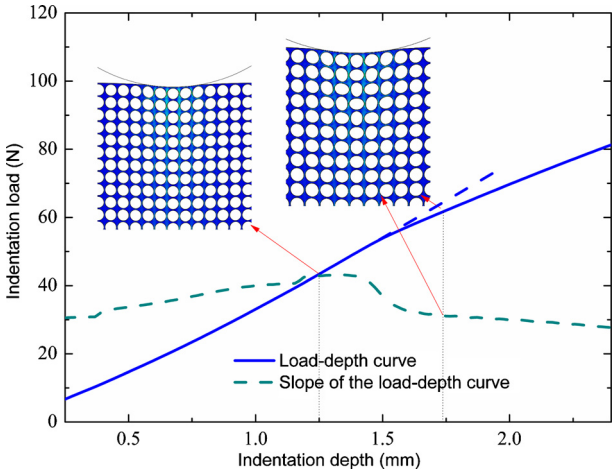

Fig. 2. (Color online.) Elastic instability in microstructure leads to a significant reduction in the slope of the indentation loading curve, where the porosity is 0.65.

pattern transformation in a rectangular region beneath the indenter. The width of the pattern transformation region scales with the contact width. The depth to which the instability propagates depends on the indentation depth. The greater the indentation depth, the more deeply the instability propagates. Since the sample is made of a highly elastic elastomer, the deformation process is purely elastic and thus completely reversible and repeatable. Upon removing the indenter, the sample can recover its original configuration.

3. Theoretical analysis and finite-element simulations

Nonlinear finite-element simulations are further performed to investigate the microstructural instability behavior in the indented elastomeric cellular material. Commercial finite-element software ABAQUS [19] is adopted. In our simulations, the indenter is assumed to be rigid because the elastic modulus of the glass indenter is much higher than that of the PDMS substrate. Around 50,000 eight-node plane-strain hybrid elements (CPE8RH) are used to model the cellular solid. The finite-element model fully copies the geometry of the experimental sample. Here the positions of a representative material point in the initial and the current configurations are described by $\mathbf{X}$ and $\mathbf{x}$, respectively. The incompressible neo-Hookean model with strain energy function $W = \frac{1}{2}\mu(\alpha_1^2+\alpha_2^2+\alpha_3^2-3)$ was used to characterize the hyperelastic constitutive behavior of the matrix material, where α_i $(i = 1, 2, 3)$ represents the principal stretch of the elastic deformation in the x_i direction, μ is the shear modulus of the matrix material and taken to be 0.5 MPa. It is noted that in a displacement-controlled indentation, the deformation of the indented solid is independent of the shear modulus and, therefore, the value of μ does not interfere with the calculation results. This can also be understood by the following dimensional analysis [20]. For a given microstructure, dimensional analysis [20] shows that the displacement, $\boldsymbol{u} = \mathbf{x} - \mathbf{X}$, at an arbitrary point x_i $(i = 1, 2, 3)$ in the indented cellular solid with circular holes can be expressed as $u_i = h\Pi(\frac{x_i}{h}, \nu, \frac{R}{h}, \frac{r}{h})$, where R is the radius of the cylindrical indenter, r the radius of each circular hole, h the indentation depth, and ν the Poisson ratio of the matrix material. It is clear that the shear modulus does not come into play. The occurrence and evolution of elastic instability in the indented material is tracked by using a pseudo-dynamic method, which has been applied in previous post-buckling analysis [21–23]. The key idea behind this nonlinear solution method is similar to the Tikhonov regularization method used to deal with ill-posed inverse problems, as discussed in Cao and Hutchinson [23]. Fig. 1b illustrates the numerical results for the deformation in the indented cellular solid from at the same indentation depth as that in Fig. 1a. A good agreement is found between the computational and the experimental results. Therefore, the present numerical simulation method can be adopted to explore other cases with different geometries and porosities. Both experiments and finite-element simulations indicate that microstructural instability will occur in the region beneath the indenter when the indentation depth reaches a critical value. Although the width of the pattern transformation region can be estimated from the contact width, two questions still remain to be answered. 1) When will the microstructural instability happen? 2) How can we predict the depth to which the instability will propagate under a given indentation depth?

To answer the first question, we carefully examine the influence of microstructural instability on the indentation force-displacement curve. Fig. 2 illustrates the loading curve of the cylindrical indenter indenting into a cellular solid with a porosity of 0.65. Distinctly, the occurrence of local instability leads to a significant reduction in the slope of the indentation load–depth curve. This phenomenon is also steadily observed for other hole geometries (e.g., elliptical) and porosities. Since the indentation load–depth curve can be directly recorded in experiments with a commercial instrument, the critical contact depth/load at the onset of microstructural instability and pattern transformation can be evaluated from the variation of the slope of the indentation loading curve.

Bearing the second aforementioned question in mind, we suggest a method to qualitatively estimate the maximum depth to which the instability propagates in the indented elastomeric cellular material with a given microstructure. Homogenization assumption is made for the indented porous substrate, which is reasonable provided that the contact radius be much larger than the characteristic size of microstructure (e.g., the hole's radius). The strain field in the homogenized indented solid is estimated using a Hertzian solution in the elastic contact theory developed for a homogeneous substrate [13]. For a cylindrical indenter indenting into an elastic half-space, the Hertzian solution gives the stresses along the line of $x_1 = 0$ as

$$\sigma_{11} = -\frac{p_0}{a}\left[\left(a^2 + 2x_2^2\right)\left(a^2 + x_2^2\right)^{-\frac{1}{2}} - 2x_2\right] \tag{1a}$$

$$\sigma_{22} = -p_0 \frac{a}{x_2}\left[\left(\frac{a}{x_2}\right)^2 + 1\right]^{-\frac{1}{2}} \tag{1b}$$

where

$$p_0 = \left(\frac{PE^*}{\pi R}\right)^{1/2} \tag{2}$$

The correlation between the indentation load P and the contact radius a is:

$$P = \frac{\pi a^2 E^*}{4R} \tag{3}$$

where the plane-strain elastic modulus $E^* = E/(1 - \nu_s^2)$. It can be noted that for the microstructure under study, the in-plane modulus exhibits certain degree of anisotropy [24]. For simplicity, the isotropic assumption is adopted in the theoretical analysis, and the elastic modulus does not come into play in the final result, as shown in the sequel. In addition, the prediction of the Poisson ratio of the porous material, ν_s, is by no means trivial, especially after the occurrence of cell buckling [24]. As can be seen from Eq. (1), in the region beneath the contact zone, especially when $x_2 > 0.5a$, the stress component σ_{22} is much larger than σ_{11}. Thus the effect of ν_s on the determination of ε_{22} is insignificant and thus we here take $\nu_s = 0$. Under these conditions, Eqs. (1)–(3) give the strain component ε_{22} along $x_1 = 0$ in the homogenized substrate as

$$\varepsilon_{22} = -\frac{a^2}{2R}\left(a^2 + x_2^2\right)^{-\frac{1}{2}} \tag{4}$$

We then consider the uniform compression of a periodic cellular elastomer as illustrated by Fig. 3a. Dimensional analysis [20] argues that for the given microstructure and boundary conditions, the critical compressive strain ε_c for the onset of microstructural instability depends only on the porosity γ, that is, $\varepsilon_c = \psi(\gamma)$. Herein the compressive strain is defined as the compressive amount divided by the original length of the sample. ψ is a dimensionless function and has been determined using finite-element simulations. Linear perturbation analysis using "Buckle" function in ABAQUS [19] is performed. Fig. 3b shows the critical buckling mode, and Fig. 3c gives ε_c as a function of porosity for different cell numbers.

Based on Eq. (4) and the critical compressive strain given in Fig. 3c, we can roughly estimate the depth of the pattern transformation region as:

$$x_{2,m} = a\sqrt{\frac{a^2}{4R^2\varepsilon_c^2} - 1} \tag{5}$$

It is noted that ε_c is very small when the void fraction is large. Thus, for the case of $\frac{a^2}{4R^2\varepsilon_c^2} \gg 1$, Eq. (5) gives the following simple scaling relation

$$x_{2,m} \sim \frac{a^2}{2R\varepsilon_c} \tag{6}$$

Fig. 4a illustrates a cellular substrate with the porosity of 60% under the indentation using a cylindrical indenter. Fig. 4b compares the values of $x_{2,m}$ predicted by Eq. (6) with those obtained from finite-element simulations. A qualitative instead of quantitative agreement is observed, demonstrating that the simple scaling relation given above could provide a rough estimation of the depth of the transformation region. A more accurate prediction may be achieved from such finite-element analysis than using the finite-element model presented here. Both Fig. 4b and Eq. (6) show that the determination of ε_c is important for the estimation of $x_{2,m}$. For the example given in Fig. 4, we take the data when around ten cells are within the contact region. In this case, only a few cells in the vicinity of $x_{2,m}$ will buckle (Fig. 4b). Therefore, it is reasonable to take a block with 5×5 or 7×7 holes to evaluate ε_c. Provided that the indenter radius is much larger than the cell size, and for instance the contact region contains tens or hundreds of cells (computational modeling of such an example is extremely time-consuming and not examined here), it is suggested to take a block (Fig. 3a) consisting of more cells to determine ε_c. But it should be noted that the results converge as shown in Fig. 3c when the cell numbers are greater than 20×20.

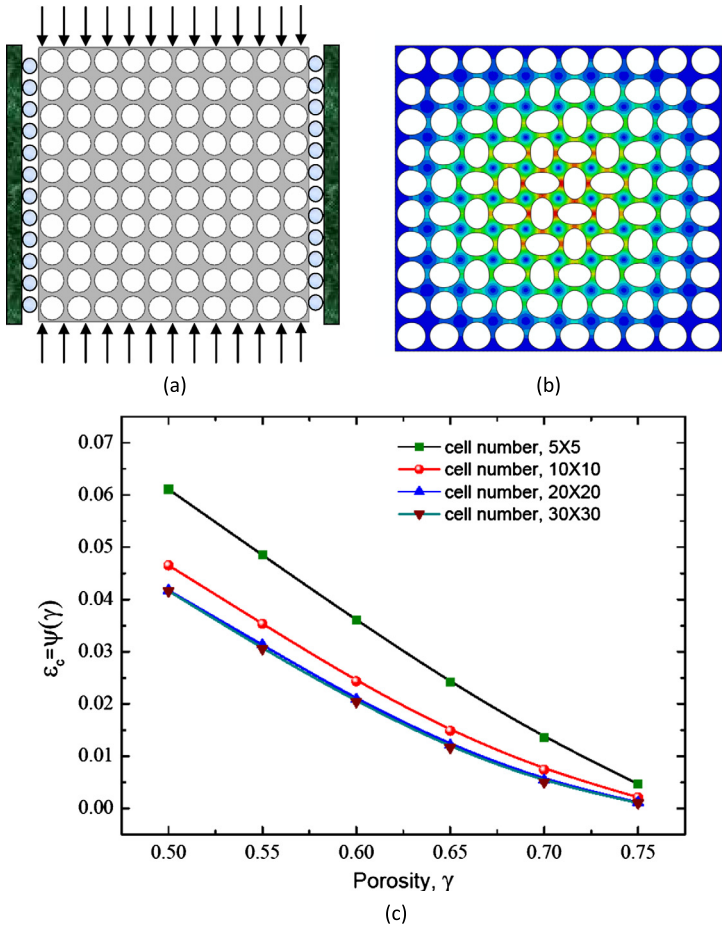

Fig. 3. (Color online.) Critical compressive strains for the onset of pattern transformation. (a) Computational model for the linear perturbation analysis (the model with 10×10 cells is chosen as an illustration); (b) critical buckling mode; (c) variation of the critical strain with the size of the model and the porosity.

Additionally, our computational results revealed that the deformation behavior of cellular elastomers is fundamentally different from that of metallic porous materials, e.g. nanoporous Au. In nanoporous Au under indentation, the buckling and crashing of cell walls were confined to a small region beneath the indenter [25]. However, the microstructure instability in elastomeric cellular solids under indentation can propagate along the depth direction in the substrate and lead to dramatic pattern transformation in an approximately rectangular region (Fig. 4a). This feature inspires some important applications of elastomeric cellular solids based on microstructural buckling techniques as mentioned above. The above analysis focuses on plane strain indentation and it is expected that the results and conclusions could provide insights into the three-dimensional cases. Besides indentation, other loading procedure, e.g. pipette aspiration [26,27], could also generate local deformation and further trigger pattern transformation with spatial gradient. This issue deserves further investigation.

4. Concluding remarks

In summary, the indentation-induced microstructural instability in elastomeric cellular solids has been explored through combined numerical, experimental, and theoretical efforts. Our study reveals that indentation-triggered pattern transformation with spatial gradient occurs within an approximately rectangular region beneath the indenter. This interesting phenomenon foresees interesting fabrication routes of advanced functional materials with switchable optical, acoustic and wetting properties. The onset of instability leads to a marked reduction in the slope of the indentation load–depth curve, which could be used to judge the occurrence of the instability. The width of the rectangular region scales with the contact width. We have presented a simple scaling relation to estimate the maximum depth to which the microstructural instability can propagate. Such a scaling relation is derived based on the homogeneous assumption of the indented solid. The assumption is reasonable when the contact radius is much larger than the typical size of the microstructure, but it is strong when instability occurs. Therefore, our simple method can only provide a qualitative estimation on the propagation depth. A quantitative evaluation of the maximum depth to which the microstructural instability propagates may be achieved from a time-consuming finite-element analysis.

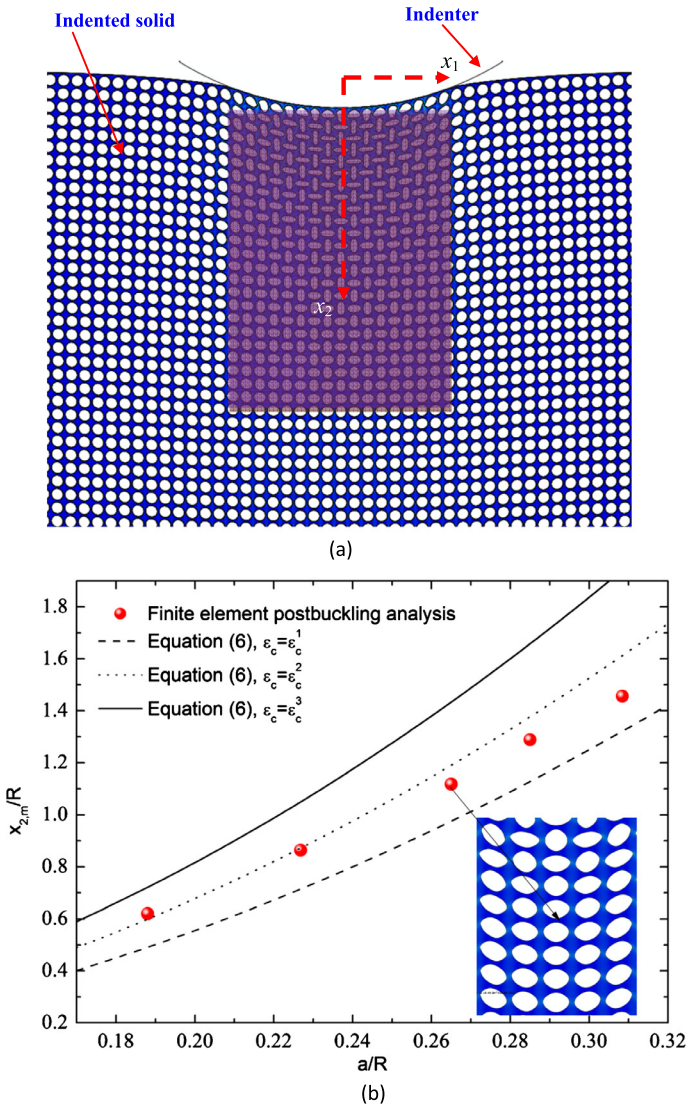

Fig. 4. (Color online.) Estimation of the maximum depth of the pattern transformation region. (a) Indentation-triggered pattern transformation for a cellular solid with a porosity of 0.60. (b) Comparison of the maximum depth predicted by Eq. (6) with finite-element simulation results. $\varepsilon_{c,1}$, $\varepsilon_{c,2}$ and $\varepsilon_{c,3}$ are determined from Fig. 3c, corresponding to the blocks with 5×5, 7×7 and 10×10 cells, respectively. $\varepsilon_{c,2}$ is given by the interpolation of the results in Fig. 3c.

Acknowledgements

Financial supports from the National Natural Science Foundation of China (Grant Nos. 10972112 and 11172155) and Tsinghua University (2012Z02103) are gratefully acknowledged.

References

[1] M. Campbell, D.N. Sharp, M.T. Harrison, R.G. Denning, A.J. Turberfield, Fabrication of photonic crystals for the visible spectrum by holographic lithography, Nature 404 (2000) 53.
[2] G.M. Whitesides, The origins and the future of microfluidics, Nature 442 (2006) 368.
[3] K. Toohey, N. Sottos, J. Lewis, J. Moore, S. White, Self-healing materials with microvascular networks, Nat. Mater. 6 (2007) 581.
[4] M. Ford, J. Bertram, S. Hynes, M. Michaud, Q. Li, M. Young, S. Segal, J. Madri, E. Lavik, A macroporous hydrogel for the coculture of neural progenitor and endothelial cells to form functional vascular networks invivo, Proc. Natl. Acad. Sci. USA 103 (2006) 2512.
[5] S. Hollister, Nat. Mater. 4 (2005) 518.
[6] S.Q. Cai, K. Bertoldi, H.M. Wang, Z.G. Suo, Porous scaffold design for tissue engineering, Soft Matter 6 (2010) 5770.
[7] T. Mullin, S. Deschanel, K. Bertoldi, M.C. Boyce, Pattern transformation triggered by deformation, Phys. Rev. Lett. 99 (2007) 084301.
[8] L.J. Gibson, M.F. Ashby, G.S. Schajer, C.I. Robertson, The mechanics of two-dimensional cellular materials, Proc. R. Soc. Lond. A 382 (1982) 25.
[9] L.J. Gibson, M.F. Ashby, Cellular Solids: Structure and Properties, 2nd edition, Cambridge University Press, 1997.

[10] D. Okumura, N. Ohno, H. Noguchi, Post-buckling analysis of elastic honeycombs subject to in-plane biaxial compression, Int. J. Solids Struct. 39 (2002) 3487.
[11] J.C. Michel, O. Lopez-Pamies, P. Ponte Castaneda, N. Triantafyllidis, Microscopic and macroscopic instabilities in finitely strained porous elastomers, J. Mech. Phys. Solids 55 (2007) 900.
[12] K. Bertoldi, M.C. Boyce, S. Deschanel, S.M. Prange, T. Mullin, Mechanics of deformation-triggered pattern transformations and superelastic behavior in periodic elastomeric structures, J. Mech. Phys. Solids 56 (2008) 2642.
[13] K.L. Johnson, Contact Mechanics, Cambridge University Press, Cambridge, UK, 1985.
[14] V. Karageorgiou, D. Kaplan, Porosity of 3D biomaterial scaffolds and osteogenesis, Biomaterials 26 (2005) 5474.
[15] W.C. Oliver, G.M. Pharr, Measurement of hardness and elastic modulus by instrumented indentation: advances in understanding and refinements to methodology, J. Mater. Res. 19 (2004) 3.
[16] S. Zankovych, T. Hoffmann, J. Seekamp, J.-U. Bruch, C.M. Sotomayor Torres, Nanoimprint lithography: challenges and prospects, Nanotechnology 12 (2001) 91.
[17] N. Fleck, H. Otoyo, A. Needleman, Indentation of porous solids, Int. J. Solids Struct. 29 (1992) 1613.
[18] M. Wilsea, K.L. Johnson, M.F. Ashby, Indentation of foamed plastics, Int. J. Mech. Sci. 17 (1975) 457.
[19] K. Hibbit, ABAQUS analysis user's manual, 2008, Version 6.8.
[20] G.I. Barenblatt, Scaling, Self-similarity and Intermediate Asymptotics, Cambridge University Press, Cambridge, UK, 1996.
[21] N. Stoop, F.K. Wittel, M. Ben Amar, M.M. Muller, H.J. Herrmann, Self-contact and instabilities in the anisotropic growth of elastic membranes, Phys. Rev. Lett. 105 (2010) 068101.
[22] B. Li, F. Jia, Y.P. Cao, X.Q. Feng, H. Gao, Surface wrinkling patterns on a core-shell soft sphere, Phys. Rev. Lett. 106 (2011) 234301.
[23] Y.P. Cao, J.W. Hutchinson, From wrinkles to creases in elastomers: the instability and imperfection-sensitivity of wrinkling, Proc. R. Soc. A 468 (2012) 94.
[24] L.J. Gibson, Biomechanics of cellular solids, J. Biomech. 38 (2005) 377.
[25] J. Biener, A.M. Hodge, A.V. Hamza, L.M. Hsiung, J.H. Satcher, Nanoporous Au: a high yield strength material, J. Appl. Phys. 97 (2005) 024301.
[26] T. Aoki, T. Ohashi, T. Matsumoto, M. Sato, The pipette aspiration applied to the local stiffness measurement of soft tissues, Ann. Biomed. Eng. 25 (1997) 581.
[27] M.G. Zhang, Y.P. Cao, G.Y. Li, X.Q. Feng, Pipette aspiration of hyperelastic compliant materials: theoretical analysis, simulations and experiments, J. Mech. Phys. Solids (2014), in press.